

Decomposition of Nitrous Oxide on Palladium Crystal Planes

BY DANIEL D. ELEY,* ANTHONY H. KLEPPING AND PETER B. MOORE

Chemistry Department, Nottingham University, University Park, Nottingham NG7 2RD

Received 24th January, 1985

The catalysed decomposition of N_2O in the range 830–1000 K and 0.05–1.0 Torr (1 Torr \approx 133 Pa) has been examined on Pd single-crystal surfaces and polycrystalline wires and compared with earlier work. The relative reaction velocities at 1000 K and 0.2 Torr are as follows: 0.01 cm diameter wire, 21; 0.025 cm diameter wire, 10.9; (610) plane, 2.2; (100) plane (thin disc), 1.8; (110) plane, 1.8; (100) plane (normal thickness disc), 1.7; and (111) plane, 1.0. Kinetic equations describing the first-order inhibition in oxygen pressure derived earlier by Eley and Knights for O_2 chemisorbed as molecules have been rederived in terms of an adsorption-desorption reaction between chemisorbed oxygen atoms and 'transitional' or 'subsurface' oxygen atoms. The apparent activation energies for Pd (and for the earlier PdAu wires) have been discussed in terms of this mechanism. From the above, 'stepsites' on (610) furnish sites *ca.* 2.7 times more active than terrace sites on (100), while grain boundaries may well be responsible for the more active sites on the Pd wires. By implication, since pure Au is known to show negligible chemisorption of O_2 at 1000 K, it seems possible that grain boundaries furnish the only active sites for N_2O decomposition on that metal.

In an earlier paper Eley and Knights¹ studied the decomposition of N_2O on a series of 17 cm \times 0.0106 cm diameter (42 s.w.g.) PdAu wires over the whole range of composition. Changes in kinetic parameters occurring around 40% Pd 40Pd 60Au were related to an 'electronic factor', namely the disappearance of 'holes in the *d*-band', which according to the old rigid-band theory occurs at this alloy composition. Here we present further studies of the catalyst kinetics of N_2O on Pd, this time in relation to any possible 'geometric factor'. To this end we have studied a 9 cm \times 0.025 cm diameter Pd wire and a series of slices cut from a Pd single crystal and exposing the close-packed (111) plane, the (100) and (110) planes and the stepped (610) plane. Because of the relatively short and thick Pd wire and the corresponding importance of end-losses of heat to the leads, it was necessary to study the temperature gradient along the wire and to devise a method of correcting the activation energies and pre-exponential factors for this.²

In this paper we use the results of surface science to help interpret the results achieved in catalysis by Pd wires, and we extend the discussion to our earlier studies on Au wires. In terms of modern concepts of surface ensembles the distinction between 'electronic' and 'geometric' factors has become rather indistinct, but the role of steps and surface defects is of great current interest in catalysis, and we are led to postulate, as a working hypothesis, a possible role for grain boundaries as active sites for the catalytic decomposition of N_2O on Pd wires. We have further postulated, as a second working hypothesis, a revision of our earlier kinetic mechanism to take account of recent knowledge of the two forms of chemisorbed oxygen atoms on Pd.

EXPERIMENTAL

APPARATUS

The reaction vessel was a Pyrex glass cylinder, diameter 3.8 cm, closed at the bottom, and attached at the top to a 7 cm diameter stainless-steel demountable flange which carried a 1.5 cm diameter water-cooled glass tube through which passed four heavy tungsten leads. Two leads were used to carry the iron heater support rods for the crystal slice, or alternatively carried the axially stretched 9 cm long Pd wire. The other two leads carried the 0.01 cm diameter wires of the Pt/Pt 13% Rh thermocouple. The Pd crystal slice was spot-welded to two 0.15 cm lengths of 0.01 cm diameter Pd wire, attached to the iron rods and used for resistive heating. The thermocouple was spot-welded to the middle of the crystal slice or to the middle of the Pd wire. It was also used to establish the temperature gradient along the catalyst wire.² The effective volume of the reaction system, as calibrated by He or N_2O gas expansion was 812.5 cm³.

The reaction vessel was connected (a) *via* a bakeable ultrahigh-vacuum (u.h.v.) leak valve to an ordinary high-vacuum gas-handling section, (b) *via* a bakeable wide-bore u.h.v. valve to the pumps, (c) *via* a branch containing a Metrosil leak to an A.E.I. MS10 mass spectrometer and (d) *via* a branch to an M.K.S. Baratron recording manometer operating in the range 0–10 Torr (1 Torr \approx 133 Pa).

The whole reaction system was bakeable at 250 °C, to given an ultimate vacuum of 5×10^{-10} Torr, which was regularly monitored by a Mullard IOG22 ion gauge on the pumping side of bakeable valve (b). The residual pressure arose mainly from CO. The use of oil-diffusion pumps lowered the possibility of mercury contamination of the catalysts.

CATALYSTS

The polycrystalline Pd wire, 9 cm long and 0.25 mm in diameter, was obtained as spectrographically pure from Johnson Matthey Ltd. The total impurities, mainly Fe, Si, Ca and Au, were < 12 ppm. The single-crystal disc was cut from a Pd single crystal, a 2.5 cm \times 0.5 cm diameter rod of 5N purity, supplied by Metals Research Ltd. The crystal was aligned to within $\pm 2^\circ$ of the desired orientation by Laue back-reflection, and slices of ca. 0.15 cm thickness cut from the crystal by spark erosion. The low-index slices were connected to a Bond barrel holder and further aligned to $\pm 0.25^\circ$ using an X-ray diffractometer. Both faces of each slice were spark-machined to give faces parallel to the desired orientation, spark techniques being used throughout to secure strain-free surfaces. Slices were subsequently electropolished in molten NaCl at 1300 K and a current density slightly greater than 1 A cm⁻².³ After 30–60 s the electrodes were raised and the crystal quenched in cold water, followed by rinsing and microscopical examination which showed the surface to be largely bright all over. Checking with LEED showed that, after annealing, the surfaces became flat on the atomic scale. The catalyst slices or wires were degreased in ether and acetone and finally rinsed in deionised water before mounting in the reaction vessel. The crystal slices, with their face (both sides) and edge areas in mm² are as follows; (110) 39, 16; (100) 36, 12; (100) thin 35, 5; (610) 35, 13 and (111) 37, 15. The edge areas formed 25–29% of the total areas apart from the (100) thin disc, for which the value was 12%.

The single-crystal slices and the Pd wire were heated resistively using an electronic control unit similar to that described earlier.⁴ The catalysts could be heated at a chosen linear rate up to a steady preset resistance (temperature) value.

REACTION PROCEDURE

After bakeout the catalyst was oxidised in 10^{-6} Torr oxygen at 1000 K for 1 h, followed by outgassing at this temperature for at least 30 min. Auger electron spectroscopy showed the resultant surface to be atomically clean, C and S having been removed as volatile oxides. Since the N_2O reaction liberated atomic O at the surface it was effectively self-cleaning, and simple outgassing between runs maintained a reproducibly active surface.

Before a run N_2O was admitted into the Baratron reference line to give the desired reaction pressure. The N_2O was then admitted to the reaction volume to give a zero reading on the Baratron, *i.e.* the desired pressure in the vessel. As the zero reading was reached, the chart

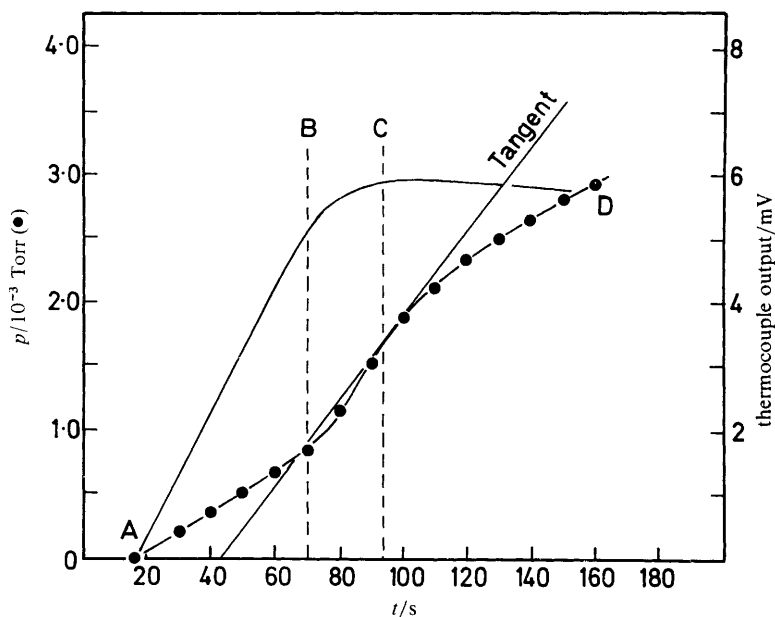


Fig. 1. The initial rate of decomposition, v_i is given by the tangent to the reaction progress curve at point C. Pd(100), 900 K, $p_{\text{N}_2\text{O}} = 2$ Torr.

recorders monitoring both manometer and catalyst thermocouples were switched on. The catalyst temperature was increased at linear rate to the desired steady value, and when this was reached, both recorder outputs were 'shorted' to put two spikes on the charts, to permit their synchronisation. The pressure-time gradient at the synchronisation point, C in fig. 1, gave the initial rate of N_2O decomposition. The effect of initial oxygen pressures (oxygen inhibition) was evaluated, as were the effects of various initial N_2O pressures. Temperature coefficients of the initial rate were determined in all cases.

RESULTS AND DISCUSSION

The initial rate, k_e , is taken as the gradient denoted in fig. 1 in Torr s^{-1} , and is converted into initial reaction velocities per unit area of catalyst, v_i , in $\text{molecule m}^{-2} \text{s}^{-1}$ by

$$v_i = k_e \frac{V}{22400} \frac{p_{\text{N}_2\text{O}}}{760} \frac{273}{298} \frac{6.023 \times 10^{23}}{A} \quad (1)$$

where V is the reaction volume in cm^3 , A is the catalyst area in m^2 , calculated from the geometry assuming a roughness factor of 1.0, and 298 K is the ambient temperature.

In table 1 we show Arrhenius parameters from plots of $\log_{10} v_i$ against T^{-1} for seven different initial pressures from 0.05 to 1.0 Torr N_2O , for the initial rates v_i , when $p_{\text{N}_2\text{O}} \rightarrow 0$, for the Pd(110) surface. A further six runs at $p_{\text{N}_2\text{O}} = 0.2$ Torr allowed us to derive a mean apparent activation energy at this pressure, with its standard deviation, $E_{\text{app}} = 97.7 \pm 1.2 \text{ kJ mol}^{-1}$. Similar sets of seven Arrhenius plots covering the range 0.05–1.0 Torr were made for the (100) and (610) discs, and single plots at

Table 1. Arrhenius parameters for Pd(110)

$p_{\text{N}_2\text{O}}$ /Torr	E_{app} /kJ mol ⁻¹	B_{m} /molecule m ⁻² s ⁻¹
0.05	104	1.26×10^{25}
0.1	99	1.01×10^{25}
0.2	98	1.45×10^{25}
0.3	100	2.70×10^{25}
0.5	97	2.34×10^{25}
0.7	93	1.75×10^{25}
1.0	84	7.94×10^{24}

0.2 Torr were made for the thin (100) disc, the (111) disc and the 0.025 cm Pd wire (standard deviation on $E_{\text{app}} \approx 1.2\sqrt{7} = 3.2$ kJ mol⁻¹).

The E_{app} values for the (110), (100) and (610) discs as a function of initial N_2O pressure, $p_{\text{N}_2\text{O}}$, are shown in fig. 2, and the values of v_1 (at 1000 K) are listed in table 2, together with the apparent frequency factors B_{m} , in the equation

$$v_1 = B_{\text{m}} \exp(-E_{\text{app}}/RT) \quad (2)$$

(all at $p_{\text{N}_2\text{O}} = 0.2$ Torr).

The wire data in table 2 were derived from an Arrhenius plot of the raw data for the 9 cm long, 0.025 cm diameter Pd wire. The temperatures for this wire were central temperatures measured by the thermocouple. A second corrected Arrhenius line was then drawn for this wire, the corrections being made as shown in ref. (2), in particular fig. 1(b). The wire used in ref. (2) was identical to that used here, *i.e.* 9 cm long, 0.025 cm diameter Pd; it was wrongly described as 32 s.w.g., *i.e.* 0.0274 cm diameter, in the earlier paper. Besides this correction for the temperature gradient, the additional correction made here, based on experimental observation, was that the fraction of surface below 800 K was poisoned by adsorbed oxygen. As in ref. (2), the main effect of the temperature gradient was to change a central-temperature activation energy, designated there as E' , of 147 kJ mol⁻¹ to a corrected activation energy E of 134 kJ mol⁻¹. The main effect of ignoring the surface fraction of the wire below 800 K was in correcting the central temperature derived, B'_{m} , to give B_{m} . Thus in ref. (2) the no-poisoning assumption gave $B'_{\text{m}}/B_{\text{m}} = 0.76$, as may be seen by reference to table 1 of that paper, whereas ignoring the $T < 800$ K surface fraction yields $B'_{\text{m}}/B_{\text{m}} = 1.43$. Thus the central-temperature-derived value of B'_{m} of 8.995×10^{27} is corrected to a value of 6.290×10^{27} molecule m⁻² s⁻¹.⁵

In table 2 we also show the Arrhenius parameters for Knights' 17 cm long, 0.01 cm diameter Pd wire.^{1,6} The temperatures used here were resistance-averaged temperatures, but because this was a relatively long, thin wire, we believe the results need a negligible correction for the temperature-gradient effect. The data are in good agreement with the present corrected data for the short, thick wire, the estimated error in E_{app} for the thin wire¹ being *ca.* 8 kJ mol⁻¹.

In fig. 3 we show that the Eley and Knights'¹ reciprocal plot of $1/v_1$ against $1/p_{\text{N}_2\text{O}}$ holds for Pd(100), good straight lines giving definite intercepts on the axis. Similar plots were obtained for (110) and (610), except that the plots showed a slight curvature downwards towards the origin of the coordinates. We include in fig. 3, for comparison purposes, Knights' plot for his 0.01 cm wire at 923 K. All lines give the same intercept on the $1/v_1$ axis.

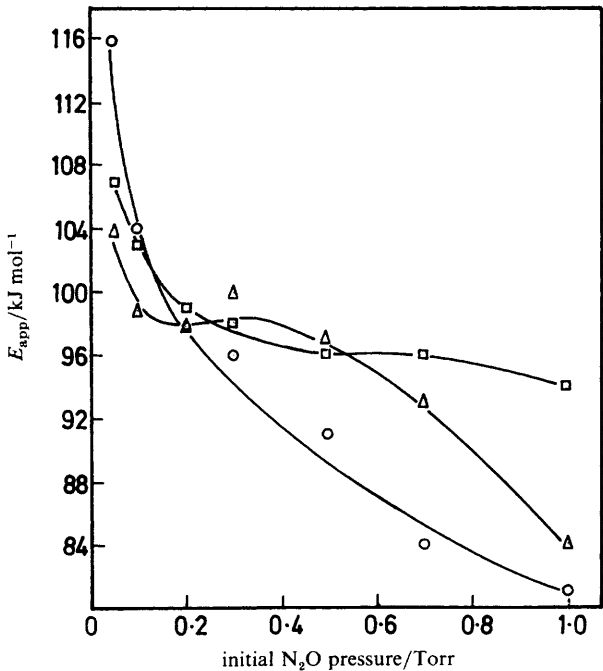


Fig. 2. Dependence of E_{app} on p_{N_2O} (no added oxygen) for \triangle , Pd(110); \square , Pd(610) and \circ , Pd(100).

Table 2. Kinetic parameters for Pd, $p_{N_2O} = 0.2$ Torr

surface	v_i , 1000 K /molecules $m^{-2} s^{-1}$	E_{app} /kJ mol^{-1}	B_m /molecule $m^{-2} s^{-1}$
wire (0.01 cm diameter) ^a	1.2×10^{21}	128	5.82×10^{27}
wire (0.025 cm diameter)	6.3×10^{20}	134	6.29×10^{27}
disc (610) plane	1.3×10^{20}	99	1.89×10^{25}
(100) thin	1.07×10^{20}	100	1.81×10^{25}
(110)	1.1×10^{20}	98	1.45×10^{25}
(100) normal	1.07×10^{20}	98	1.42×10^{25}
(111)	5.76×10^{19}	100	9.35×10^{24}

^a From ref. (1) and (16).

The effect of initially added oxygen is seen in fig. 4: $1/v_i$ varies linearly with p_{O_2} , rather than $p_{N_2O}^{\frac{1}{2}}$, for Pd(111), with a similar plot, not shown here, for the 9 cm long, 0.025 cm diameter Pd wire. This confirms the earlier result for the 17 cm long, 0.01 cm diameter Pd wire.¹ Fig. 5, again confirming Knights' work,¹ shows that the effect of added oxygen in decreasing the initial rate of N_2O decomposition is accompanied by an increase in apparent activation energy, E_{app} .

Note that in this paper when we use the terms true and apparent activation energy we are referring to the differences arising from heats of adsorption of reactants and

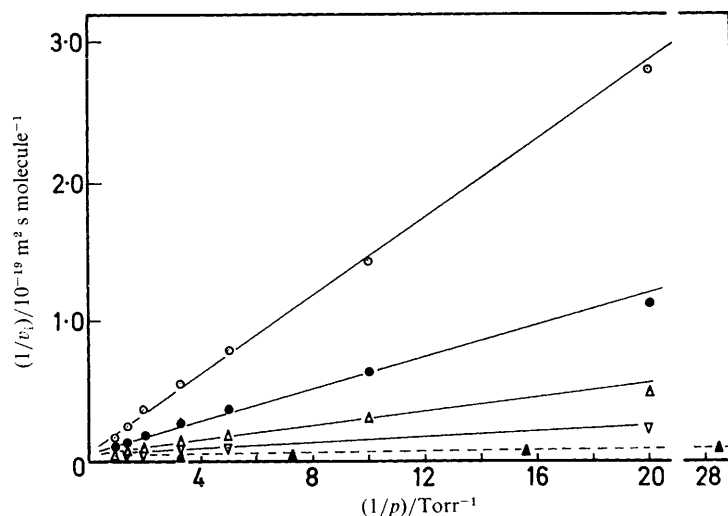


Fig. 3. Dependence of $1/v_i$ on $1/p_{\text{N}_2\text{O}}$ (no added oxygen) for Pd(100) at ∇ , 1000; \triangle , 950; \bullet , 900 and \circ , 850 K. The dotted line (\blacktriangle) is for Knights' 0.01 cm wire, at 923 K.^{1,14}

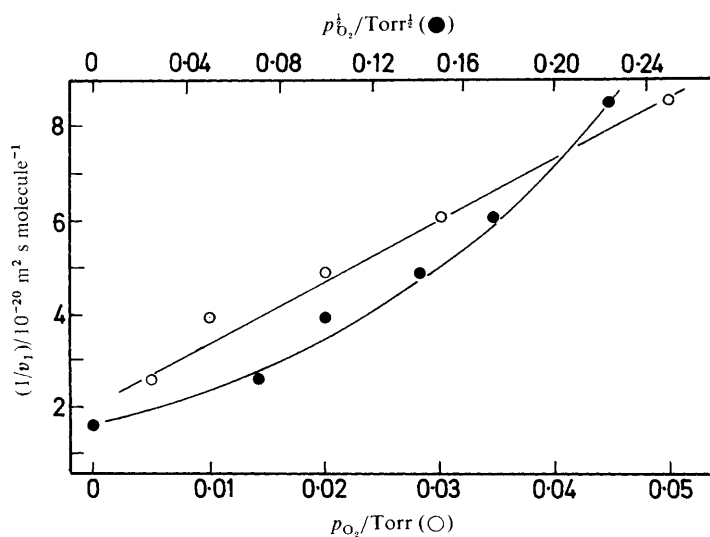


Fig. 4. Effect of added oxygen on $1/v_i$ at $p_{\text{N}_2\text{O}} = 0.2$ Torr. The linear plot (\circ) is against p_{O_2} . A similar result was found for the 9 cm long, 0.025 cm diameter Pd wire.

products, the usual distinction. We have tried to avoid this phraseology in discussing the various activation energies, E , E' and E'' , arising from temperature-gradient considerations in an electrically heated wire catalyst.²

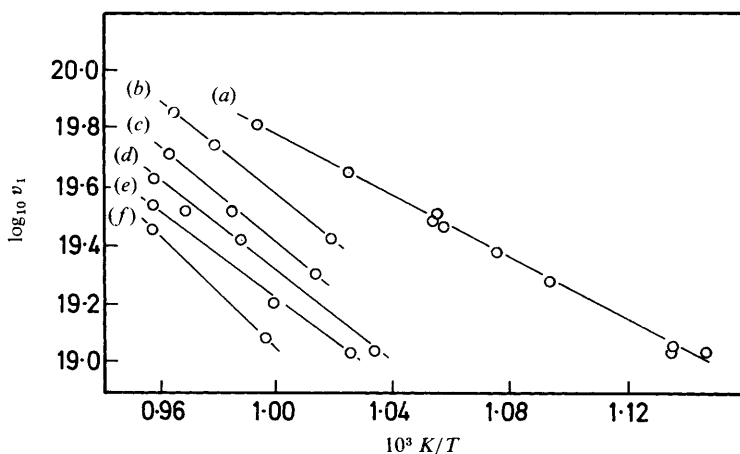


Fig. 5. Effect of added oxygen in raising E_{app} for N_2O decomposition (initial $p_{N_2O} = 0.2$ Torr) for Pd(111). A similar series of graphs were found for the 9 cm long, 0.025 cm diameter Pd wire. The added oxygen pressures, p_{O_2} , are (a) 0.0, (b) 0.005, (c) 0.01, (d) 0.02, (e) 0.03 and (f) 0.05 Torr.

ISOTOPIC NITROUS OXIDE

The rate of production of $^{14}N^{15}N$, m/e 29, from the decomposition of a mixture of equal volumes of $^{14}N^{14}NO$ and $^{15}N^{15}NO$ was examined on the 9 cm long, 0.025 cm diameter Pd wire at 1050 K and at 0.5, 0.8 and 1.0 Torr initial pressures of N_2O . Less than 1% of m/e 29 is produced during a reaction time of 800 s, and this small amount probably comes from reaction on the mass-spectrometer filament. We conclude there is no $N\equiv N$ bond fission in the N_2O decomposition on Pd under our conditions of temperature and pressure.

KINETICS AND MECHANISM

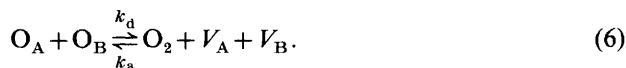
Laidler⁷ has reviewed the literature of heterogeneous catalytic N_2O decomposition, from the work of Hinshelwood and Prichard⁸ on a Pt filament in 1925, to 1951, and including the metals Pt, Au and Ag, he has proposed the general law

$$v = \frac{kp_{N_2O}}{1 + bp_{N_2O} + b'p_{O_2}} \quad (3)$$

So far as Pd is concerned, Eley and Knight¹ used this equation to describe their results on Pd and PdAu filaments, as did Redmond,⁹ the latter with $b = 0$. Riekert and Schuchmann¹⁰ observed that when the oxygen pressure formed in the N_2O decomposition exceeded the PdO dissociation pressure a layer of this oxide was formed on the metal with a greater catalytic efficiency than Pd itself. For example, at 700 °C when the O_2 pressure reached 28.1 Torr, in excess of a calculated PdO dissociation pressure of 15 Torr, the catalyst passed into a more active state. Recently Conrad *et al.*¹¹ have demonstrated the existence of a surface oxide monolayer which has a 2×2 LEED pattern similar to that of adsorbed O atoms, but which is more stable than this species and more stable than bulk PdO. On Pd(111) this stable 'transitional' oxide layer gave a shoulder at 850 °C on the thermal-desorption peak at 600 °C characteristic

of ordinary adsorbed O atoms, and it was also seen by its effect on the u.p.s. spectrum of Pd. It is probably a subsurface monolayer formed *via* surface steps or defects.¹²

Our present results, in which $1/v_i$ is linear when plotted against $1/p_{\text{N}_2\text{O}}$ for $p_{\text{O}_2} \rightarrow 0$ (fig. 3) or against p_{O_2} (rather than $p_{\text{O}_2}^{\frac{1}{2}}$, fig. 4), give a reasonable fit to eqn (3), which Eley and Knights¹ derived from a stationary-state analysis involving chemisorbed molecular oxygen, held by one and two bonds, as well as atomically adsorbed oxygen. The atomically adsorbed species, by itself, of course gives rise to $p_{\text{O}_2}^{\frac{1}{2}}$ inhibition, not found here. Here we note that the oxygen pressures involved are too small to lead to bulk PdO formation, but that under our conditions we must expect both normal adsorbed atomic oxygen, O_A , (number of sites per m^2 , N_A , fractional coverage, θ_A) and the relatively stable, probably subsurface atomic species O_B (N_B , θ_B). If V_A and V_B denote vacant sites for O_A and O_B , we have found that the analysis summarised below leads to equations of identical form for v and E_app to those of Eley and Knights.¹ The reaction sequence postulated is as follows:



The overall rate is written as

$$v = k_\text{n} N_\text{A} p_{\text{N}_2\text{O}} (1 - \theta_\text{A}). \quad (7)$$

In the stationary state $d\theta_\text{A}/dt = d\theta_\text{B}/dt = 0$ and the rate of appearance of O_2 gas is

$$v/2 = k_\text{d} N_\text{A}(\theta_\text{A}) N_\text{B}(\theta_\text{B}) - k_\text{a} p_{\text{O}_2} N_\text{A}(1 - \theta_\text{A}) N_\text{B}(1 - \theta_\text{B}). \quad (8)$$

With $b = k_\text{a}/k_\text{d}$ and $Z = 1/\theta_\text{B}$ eqn (7) and (8) yield

$$\frac{1}{v} = \frac{Z}{2k_\text{d} N_\text{A} N_\text{B}} + \left(\frac{1 + (Z-1)bp_{\text{O}_2}}{k_\text{n} N_\text{A}} \right) \frac{1}{p_{\text{N}_2\text{O}}}. \quad (9)$$

Applying the Arrhenius operator $RT^2(d \ln/dT)$ to v in eqn (9) we derive, after considerable algebra, the apparent activation energy

$$E_\text{app} = E_\text{n} - (E_\text{n} - E_\text{a}) \left(\frac{Zv}{2k_\text{d} N_\text{A} N_\text{B}} \right) + \Delta H(1 - \theta_\text{A}) bp_{\text{O}_2} \quad (10)$$

where ΔH is the enthalpy of desorption of oxygen according to eqn (6) [with sign as in ref. (1)], *i.e.* in terms of activation energies:

$$-\Delta H = RT^2 \frac{d \ln b}{dT} = E_\text{a} - E_\text{d}. \quad (11)$$

Eqn (9) and (10) transform to the corresponding equations in ref. (1) (denoted Knights) for the case of $\theta_\text{B} = 0.5$, *i.e.* $Z = 2$, by putting $S(\text{Knights}) = N_\text{A}$, $2k_\text{d}(\text{Knights}) = k_\text{d} N_\text{B}$ and $\theta_{\text{O}_2}(\text{Knights}) = \theta_\text{A}$.

The decrease in E_app with $p_{\text{N}_2\text{O}}$ in fig. 2 may be seen to arise from the second term on the right-hand side of eqn (10), involving v , which is proportional to $p_{\text{N}_2\text{O}}$. Oxygen arising during the initial decomposition (see later), operating through the third term will cause the observed deviations from linearity in fig. 2.

It now seems to us that molecularly chemisorbed O_2 is unlikely to be found on Pd at 1000 K, whereas there is definite evidence for the second rather stable form of adsorbed oxygen atoms, so that the present treatment gives a more rational basis for the observed kinetics.

KINETIC ANALYSIS APPLIED TO Pd(100)

The data in fig. 3 for Pd(100) is a sufficiently close fit to our analysis to allow a derivation of E_n . We first note that the oxygen already present at the time of measurement of the initial rate v_i (see fig. 1), if it were all adsorbed, would be sufficient to give *ca.* 200 monolayers on the Pd disc. So in any consideration of $1/v_i$ or E_{app} it is probably necessary to include the term bp_{O_2} .

The slope of the plot of $1/v_i$ against $1/p_{N_2O}$ in fig. 3 for Pd(100) gives $k_n N_A / 1 + (Z-1)bp_{O_2}$, and in fig. 6 we present an Arrhenius plot of this quantity as a function of $1/T$; a straight line results, the slope of which yields an apparent activation energy:

$$E_{app}^* = E_n + \frac{(Z-1)bp_{O_2}}{1 + (Z-1)bp_{O_2}} \Delta H. \quad (12)$$

If we assume $\theta_B = 0.5$, $Z = 2$ and $bp_{O_2}/1 + bp_{O_2} = 1 - \theta_A$, then

$$E_{app}^* = E_n + \Delta H(1 - \theta_A)bp_{O_2}. \quad (13)$$

From fig. 6 we derive $E_{app}^* = 126 \text{ kJ mol}^{-1}$. The intercept on fig. 3, common for all four temperatures, is given according to eqn (9) as

$$\frac{1}{k_d N_A N_B} \approx \frac{Z}{2k_d N_A N_B} = 16.6 \times 10^{19} \text{ molecules m}^{-2} \text{ s}^{-1}.$$

Again, on the assumption $Z = 2$,

$$E_{app}^* - E_{app} = \frac{(E_n - E_a)v}{k_d N_A N_B}.$$

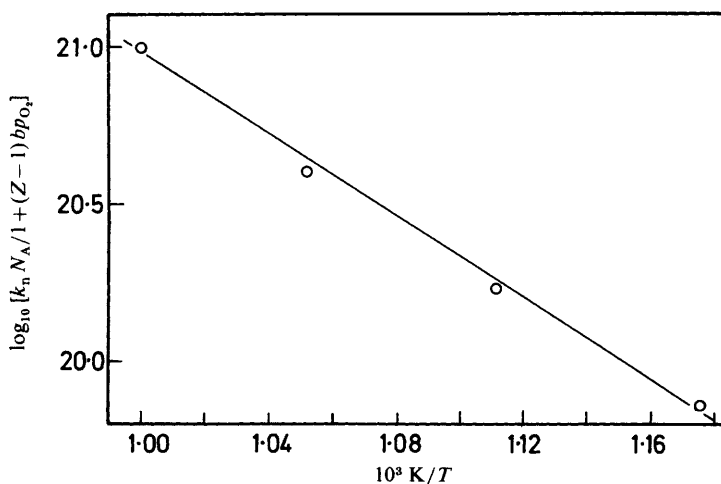


Fig. 6. Arrhenius plot of the logarithm of the slope of the graph in fig. 3, *i.e.*

$$\log_{10} [k_n N_A / 1 + (Z-1)bp_{O_2}], \text{ against } T^{-1}.$$

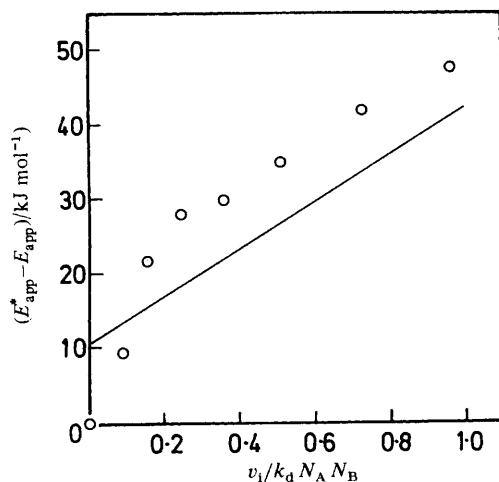


Fig. 7. Plot of $E_{app}^* - E_{app} = 126 - E_{app}$, in $kJ mol^{-1}$, (E_{app} values from fig. 3) against $v_i / k_d N_A N_B$ for Pd(100), v_i from fig. 2 taken at $10^3/T = 1.076$. The line is a least-squares plot.

A least-squares analysis applied to fig. 7, which is a plot of $(E_{app}^* - E_{app})$ against $v_i / k_d N_A N_B$, and including the (0, 0) point gives

$$E_n - E_a \approx E_n = 43 \pm 7.2 \text{ kJ mol}^{-1}, \text{ Pd(100)}.$$

It seems reasonable to assume $E_a = 0$, *i.e.* no activation energy for the adsorption of oxygen, although this has not been demonstrated. This result is comparable to the value $E_n = 53 \text{ kJ mol}^{-1}$ derived by Eley and Knights¹ for their Pd and PdAu alloy wires, from oxygen inhibition plots at different temperatures. Unfortunately we did not obtain oxygen-inhibition plots at different temperatures in the present work. Continuing to assume $Z = 2$, from eqn (13)

$$\Delta H(1 - \theta_A) b P_{O_2} = E_{app}^* - E_n = 83 \text{ kJ mol}^{-1}$$

for Pd(100), *i.e.* the desorption term dominates the apparent activation energy, E_{app} , and it is reasonable to suppose a similar result holds for the other Pd surfaces of table 2.

CONCLUSIONS

The most close-packed plane of the Pd f.c.c. lattice is (111), and table 2 shows that relative to this plane the catalytic activities at 1000 K and 0.2 Torr N_2O are as follows: polycrystalline wire (0.01 cm diameter), 21; polycrystalline wire (0.025 cm diameter), 10.9; (610) plane, 2.2; (100) thin disc, 1.8; (110), 1.8; (100), normal disc, 1.7; and (111), 1.0. These results are similar to those of Löffler and Schmidt¹³ for the decomposition of NH_3 on Pt, and in contrast to for example, the very marked differences between single-crystal surfaces of Re in NH_3 synthesis.¹⁴ A consideration of the present stepped (610) surface, considered as a (100) surface with monatomic steps at intervals of 6 atoms suggests each step site to be about 2.7 times as active as a site on the (100) plane. The wires, however, are noticeably more active than the single-crystal surfaces. On energetic grounds the exposed planes are expected to be (111), (100) and (110), which clearly cannot account for the effect themselves. Knights⁶ found that under the optical

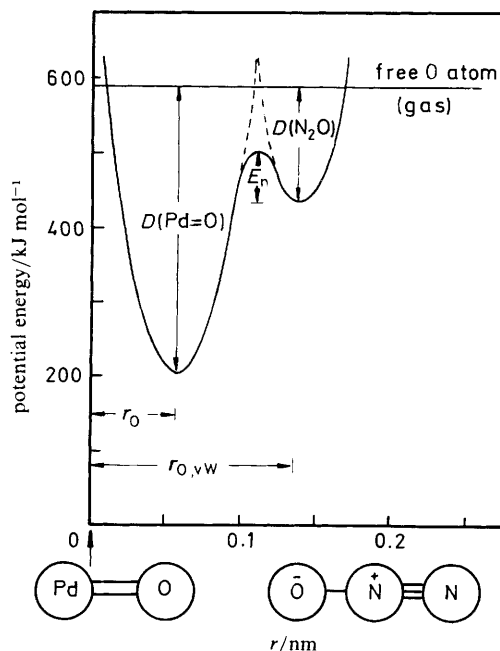


Fig. 8. Potential-energy curves, sketched as in the text, for the O-atom transfer $\text{N}_2\text{O} + \text{Pd} \rightarrow \text{Pd}=\text{O} + \text{N}_2$.

microscope a new Pd filament showed no crystalline structure, but on annealing at 800–900 °C for 3 h *in vacuo* ($< 10^{-6}$ Torr) developed a well defined structure of grain boundaries which showed no further change in crystallite size even after extensive use in N_2O decomposition. While the width of grain boundary channels at c (0.5 nm) is much less than that of a grain, some 5×10^4 nm,¹⁵ the sites in grain boundaries are expected to be especially reactive, and so it would appear for the N_2O decomposition. The higher E_{app} values for the wires we might reasonably associate with a higher enthalpy of desorption of oxygen, the dominance of which came out of the previous kinetic analysis. The 10^4 -fold decrease in wire activity from Pd to 40Pd60Au found by Eley and Knights¹ is clearly unlikely to arise from simple lattice-plane effects. However, a modern view (as recently given for the reaction between CO and O_2) would tend to correlate the rate with the presence of surface Pd_{9+1} ensembles, rather than with 'holes in the d -band'.⁴ In addition, we have noted⁴ that some Au-rich alloys (1.5Pd98.5Au was cited, but not pure Au) form stable surface oxides at 1000 K, in which case an additional inhibitory factor would be present.

The idea that $E_n \approx 50$ kJ mol⁻¹ is made plausible by reference to the potential-energy curves of fig. 8. These show that the crossing-point for transfer of an O atom from N_2O striking the surface vertically to form surface PdO would reasonably occur around this E_n value. In sketching this diagram we have ignored any van der Waals adsorption energy and zero-point energy effects for the vibrations. To draw the $\text{Pd}=\text{O}$ curve we have used a heat of chemisorption of 280 kJ mol⁻¹¹⁶ to calculate a bond dissociation energy $D(\text{Pd}=\text{O})$ of 389 kJ mol⁻¹ and an estimated force constant (from Cottrell's data¹⁷) of 5.7×10^5 dyn cm⁻¹. For N_2O we took $D(\text{N}_2=\text{O}) = 159$ kJ mol⁻¹ and an estimated force constant of 6×10^5 dyn cm⁻¹. The double-bond radius of the

O atom $r(\text{=O})$ of 0.057 nm, and its van der Waals radius $r_{\text{O, vW}}$ of 0.14 nm, are taken from Pauling.¹⁹ According to the arguments of the earlier paper¹ this model should hold from Pd to 55Pd45Au, gold and gold-rich alloys requiring additional discussion in terms of the involvement of defect sites in the surface.

Considering the case of pure Au, the electron-spectroscopic observation that this metal does not chemisorb any appreciable amount of O_2 under u.h.v. conditions, even at 1000 K,²⁰ has now been confirmed.^{21, 22} The small amounts of O_2 that were taken up were due to surface contaminants, such as Si.^{21, 22} It is therefore unlikely that N_2O decomposition on Au wires occurs on the lattice planes, and we are led back to the earlier view⁴ that it must occur on defect sites. In view of the present results it seems reasonable to suggest that grain boundaries may be the sites at which N_2O adsorbs and decomposes on polycrystalline Au. How far impurity atoms, which would tend to concentrate at grain boundaries, are involved, must await further evidence. It is possible that the much higher E_{app} value observed by Hinshelwood and Prichard for their Au wire,²³ compared with that found by Eley and Knights,¹ may arise from impurity effects. It would appear that the Au wire of ref. (23) was exposed to the vapour of liquid Hg at 0 °C, whereas that used in ref. (1) was protected by a trap at -78 °C.

The mechanism we have advanced above for Pd at low N_2O pressures may be worthy of consideration wherever first-order oxygen inhibition and 'subsurface' oxygen are found. Classical Langmuir-Hinshelwood kinetics, involving recombination of 2O_A and $p_{\text{O}_2}^{1/2}$ inhibition, has been found for low-pressure N_2O on Pt.²⁴⁻²⁶ At higher pressures of N_2O on Pt the reaction $\text{N}_2\text{O} + \text{O}_\text{A}$ can play a dominating role.²⁷ The mechanism of Eley and Knights,¹ involving two clearly defined stages of molecular O_2 chemisorption, although *a priori* unlikely on Pd at 1000 K, may well be applicable to N_2O decomposition on appropriate catalysts at lower temperatures*.

The relatively small surface-plane sensitivity of N_2O on Pd mentioned in this paper, and NH_3 decomposition on Pt,¹³ as compared with NH_3 synthesis on Re¹⁴ referred to earlier, probably reflects a simple single-coordinate link formed in the chemisorption of N_2O or NH_3 , compared with the need to disrupt the $\text{N}\equiv\text{N}$ triple bond on two adjacent highly unsaturated metal sites in the case of the last named reaction.

D. D. E. thanks the Leverhulme Trust for the award of an Emeritus Fellowship.

* *Note added in proof.* This requires reconsideration in view of the new findings of $p_{\text{O}_2}^{1/2}$ rather than p_{O_2} inhibition for Pt and Rh.²⁸

¹ D. D. Eley and C. F. Knights, *Proc. R. Soc. London, A*, 1966, **294**, 1.

² D. D. Eley, A. H. Klepping and P. B. Moore, *J. Chem. Soc., Faraday Trans. 1*, 1983, **79**, 669.

³ P. R. Rowland, *Nature (London)*, 1953, **171**, 931.

⁴ D. D. Eley and P. B. Moore, *Surf. Sci.*, 1981, **111**, 325.

⁵ A. H. Klepping, *Thesis* (University of Nottingham, 1981).

⁶ C. F. Knights, *Thesis* (University of Nottingham, 1964).

⁷ K. J. Laidler, *Catalysis*, ed. P. H. Emmett (Reinhold, New York, 1954), vol. I, p. 146.

⁸ C. N. Hinshelwood and C. R. Prichard, *J. Chem. Soc.*, 1925, **127**, 327.

⁹ J. P. Redmond, *J. Catal.*, 1967, **7**, 297.

¹⁰ L. Rieckert and H. P. Schuchmann, *Ber. Bunsenges. Phys. Chem.*, 1964, **68**, 986.

¹¹ H. Conrad, G. Ertl, J. Küppers and E. E. Latta, *Surf. Sci.*, 1977, **65**, 245.

¹² D. L. Weissmann, M. L. Shek and W. E. Spicer, *Surf. Sci.*, 1980, **92**, L59.

¹³ D. G. Löffler and L. D. Schmidt, *Surf. Sci.*, 1976, **59**, 195.

¹⁴ M. Asscher and G. A. Somorjai, *Surf. Sci.*, 1984, **143**, L389.

¹⁵ P. H. Pumphrey, in *Grain Boundary Structure and Properties*, ed. G. A. Chadwick and D. A. Smith (Academic Press, New York, 1976), p. 184.

¹⁶ D. Brennan, D. O. Hayward and B. M. W. Trapnell, *Proc. R. Soc. London, A*, 1960, **256**, 81.

¹⁷ T. L. Cottrell, *The Strengths of Chemical Bonds* (Butterworths, London, 2nd edn, 1958), p. 270.

- ¹⁸ R. P. H. Gasser and D. E. Holt, *Surf. Sci.*, 1975, **52**, 457.
- ¹⁹ L. Pauling, *The Nature of the Chemical Bond* (Cornell University Press, Ithaca, 1st edn, 1939), pp. 154 and 176.
- ²⁰ D. D. Eley and P. B. Moore, *Surf. Sci.*, 1978, **76**, L599.
- ²¹ J. J. Pireaux, M. Chtaib, J. P. Delrue, P. A. Thiry, M. Liehr and R. Caudano, *Surf. Sci.*, 1984, **141**, 211.
- ²² N. D. S. Canning, D. Outka and R. J. Madix, *Surf. Sci.*, 1984, **141**, 240.
- ²³ C. N. Hinshelwood and C. R. Prichard, *Proc. R. Soc. London, A*, 1925, **108**, 211.
- ²⁴ H. Cassell and E. Glückauf, *Z. Phys. Chem. B*, 1932, **17**, 380.
- ²⁵ J. P. Redmond, *J. Phys. Chem.*, 1963, **67**, 788.
- ²⁶ C. G. Takoudis and L. D. Schmidt, *J. Catal.*, 1983, **80**, 274.
- ²⁷ L. Riekert and M. Staib, *Ber. Bunsenges. Phys. Chem.*, 1963, **67**, 976.
- ²⁸ C. G. Papapolymerou and L. D. Schmidt, *Langmuir*, 1985, **1**, 488.

(PAPER 5/138)